Journal of Neuroscience Methods 331 (2020) 108449

Contents lists available at ScienceDirect

Journal of Neuroscience Methods

journal homepage: www.elsevier.com/locate/jneumeth

Micturition video thermography in awake, behaving mice

Anne M. Verstegen[a,1], Margaret M. Tish[b,1], Luca P. Szczepanik[c], Mark L. Zeidel[c], Joel C. Geerling[b,*]

[a] Division of Endocrinology, Diabetes, and Metabolism, Department of Medicine, Beth Israel Deaconess Medical Center, Harvard Medical School, Boston, MA, 02215, USA
[b] Department of Neurology, University of Iowa Hospital and Clinics, Iowa City, IA, USA
[c] Division of Nephrology, Department of Medicine, Beth Israel Deaconess Medical Center, Harvard Medical School, Boston, MA, 02215, USA

ARTICLE INFO

Keywords:
Micturition
Urination
Void
Voiding
Void spot
Cystometrogram
Cystourethrogram
Cystourethography
Urodynamic
Bladder
Detrusor
Continence
Thermographic

ABSTRACT

Background: Our understanding of the neural circuits controlling micturition and continence is constrained by a paucity of techniques for measuring voiding in awake, behaving mice.
New method: To facilitate progress in this area, we developed a new, non-invasive assay, micturition video thermography (MVT), using a down-facing thermal camera above mice on a filter paper floor.
Results: Most C57B6/*J* mice void infrequently, with a stereotyped behavioral sequence, and usually in a corner. The timing of each void is indicated by the warm thermal contrast of freshly voided urine. Over the following 10–15 min, urine cools to ~3 °C below the ambient temperature and spreads radially in the filter paper. By measuring the area of cool contrast comprising this "thermal void spot," we can derive the initially voided volume. Thermal videos also reveal mouse behaviors including a home-corner preference apart from void spots, and a stereotyped, seconds-long pause while voiding.
Comparison with existing methods and Conclusions: MVT is a robust, non-invasive method for measuring the timing, volume, and location of voiding. It improves on an existing technique, the void spot assay, by adding timing information, and unlike the cystometrogram preparation, MVT does not require surgical catheterization. Combining MVT with current neuroscience techniques will improve our understanding of the neural circuits that control continence, which is important for addressing the growing number of patients with urinary incontinence as the population ages.

1. Introduction

Since Barrington identified the micturition reflex circuit between the spinal cord and brainstem (Barrington, 1924), our understanding of the brain circuits that control bladder function has advanced slowly. One roadblock to progress is the lack of a simple, noninvasive assay for voiding behavior that can be combined with modern neuroscience methods in awake, behaving mice. Mice are the primary species for genetically targeting cell types and circuit connections, and we have robust tools and techniques for recording specific neurons and turning them on and off with increasingly high precision. A key advantage of these techniques is that they allow experiments in awake, behaving animals, without the need for anesthesia or mechanical restraint, so ideally, we would pair these techniques with *live* assays in *unanesthetized* mice. Further, due to the nuance and variability of mouse behavior, experimental designs allowing repeat testing and within-animal controls are becoming the norm.

Unfortunately, existing bladder function assays are ill-suited for live experiments in awake, behaving mice. For example, the classic cystometrogram (CMG) preparation infuses saline into the bladder while recording changes in bladder pressure (Andersson et al., 2011; Bjorling et al., 2015). In mice, this technique requires surgical insertion of a catheter through the bladder wall, which can irritate the detrusor muscle and alter the mechanics of voiding. The CMG is typically a terminal assay with urethane anesthesia (but see Pandita et al., 2000), which alters the activity of neurons across the central nervous system (Yoshiyama et al., 1994). Our widest knowledge gaps involve continence-controlling neural circuits in the forebrain, so anesthetic drugs that inhibit these circuits represent a major barrier to progress.

Another technique, void spot analysis, places an unanesthetized, freely moving mouse atop absorbent paper for several hours (Bjorling et al., 2015; Hill et al., 2018; Sugino et al., 2008; Yu et al., 2014). Post hoc analysis of urine spots in the paper reveals the number and spatial distribution of voids, and volume can be inferred from a linear

* Corresponding author at: PBDB-1320, 169 Newton Rd., Iowa City, IA, 52246, USA.
E-mail address: joel-geerling@uiowa.edu (J.C. Geerling).
[1] These authors contributed equally.

https://doi.org/10.1016/j.jneumeth.2019.108449
Received 1 May 2019; Received in revised form 11 September 2019; Accepted 27 September 2019

relationship with the area of each void spot, but this technique offers no information about the order or timing of voids. Post hoc analysis is poorly suited for studying neural circuits, where relevant events occur on the order of milliseconds to seconds. This approach also cannot distinguish between one or multiple voids when they overlap, as occurs often in cage corners.

Newer techniques attempt to address some of these limitations. In one of these, rats or mice are housed on a metal grid, and their urine falls onto a finely calibrated scale; the resulting change in weight signals the timing and amount of each void (UroVoid, Med Associates). This approach offers temporal resolution and volume estimates, but provides no information about mouse behavior or the spatial distribution of voids. Metal grid flooring is inherently stressful to rodents, altering their behavior (Krohn et al., 2003). Also, voided urine that adheres to the metal wires is not measured. Another group of investigators used an overhead camera to track the X–Y position of a mouse and correlate that with fluorescence changes in the filter paper flooring, detected by a separate camera beneath the cage, signaling voids (Hou et al., 2016).

We wanted a simpler assay for awake, behaving mice that would allow us to record several mice simultaneously and that combines the temporal resolution of a CMG with the volume estimates and spatial information of void spot analysis. An ideal assay would be repeatable, non-invasive, and compatible with modern neuroscience techniques like optogenetics and fiber photometry. Here we describe such a technique, which we call micturition video thermography (MVT).

2. Materials and methods

Mice. We used male and female C57B6/*J* mice (8–12 weeks old; Jackson laboratories) to standardize and characterize our assay, following pilot tests with mixed-background mice from our breeding colonies. All mice were group-housed in a barrier facility with *ad libitum* access to standard rodent chow and water, except during the 2 h MVT assay. We removed mice from their cages for MVT just prior to or within 1 h of lights-off. We measured ambient temperatures in the range of 21–24 °C in our mouse housing and procedure rooms, with a background variance of less than +/- 1 °C in individual rooms. All procedures in these experiments were carried out in accordance with the NIH Guide for the Care and Use of Laboratory Animals and were approved by the Institutional Animal Care and Use Committees at BIDMC and University of Iowa.

Enclosures. For initial recordings, we used polyethylene containers from a local store (Bed, Bath, and Beyond) to assemble hinged, open-top recording chambers (base: 20 cm x 14 cm; 20 cm tall). Trial and error determined a height of roughly 20 cm as adequate to prevent most mice from climbing or jumping out of the open top. Because we observed that mice void primarily in the corners, for more recent MVT recordings we assembled enclosures from laser-cut acrylic with taller (25 cm) walls that angle outward toward the camera, improving the camera view of inner cage corners (Fig. 1C).

An open-top design was necessary because infrared radiation in the range measured by thermal cameras (long-wavelength infrared, ~8–12 μm) does not penetrate most solids, including plastic cage walls. Our attempts at recording through a grid roof or floor resulted in blocked and blurred thermal signals, which significantly compromised the accuracy of measurements. Polyvinylidine chloride (PVDC, e.g. Saran plastic wrap) did pass infrared light with only slight attenuation, equivalent to ~1-2 °C reduction in apparent temperature. However, blocking airflow with this material is not ideal for mouse ventilation, and from a practical perspective, it is difficult to place and sustain a perfectly smooth surface atop cages, and even minor ripples or snags generated haze or shimmering artifacts that obscured thermal recordings and compromised the accuracy of measurements.

Immediately prior to each test, we covered each cage floor with fresh, dry paper. This allows an estimate of voided volume from the area of diffusion as in previous reports (Hill et al., 2018; Sugino et al., 2008; Yu et al., 2014). Initial MVT recordings and calibrations were performed on standard laboratory filter paper (GB004; Whatman Inc., now GE Healthcare #10,427,922; lot #7,299,011), but we later switched to and re-calibrated the void spot area-volume relationship using blotting paper (Cosmos F36 − COSBLT12038, 360 gsm; Blick Art Supply). This paper resists shredding, which was an occasional problem with a subset of mice.

For experiments at BIDMC, we placed a chow pellet at the center of the filter paper to occupy the mouse during the 2 h recording. Mice tested at the University of Iowa (for added analysis of mouse position, locomotor behavior, and detailed temperature evolution of void spots) did not have chow during the recording. We withheld water during MVT recordings to eliminate confounds in bladder filling and voiding from inter-individual differences in water intake during the test and because bottle spillage obfuscates void spot analysis (Hill et al., 2018; Yu et al., 2014). We cleaned cages between each test with (initial cage design) 70% ethanol followed by a rinse with 50 °C water or (later, open cage design) warm water, then towel-dried and air-dried each cage to eliminate any residual liquid and allowed cages to return to ambient temperature before the next test.

Thermal imaging. We tested three different microbolometer-type thermal cameras over the course of this study. For pilot tests, we used an E40 camera augmented with a 45° field of view lens (FLIR Systems). This camera captures long-wave (8–12 μm) infrared radiation using an uncooled array of vanadium oxide sensors (320 × 240). The sensors report temperatures -20° to +650 °C, and at ambient temperatures near 30 °C can detect differences as small as 0.07 °C. Later, we switched to a higher resolution A65 camera (640 × 512 sensor array, FLIR), with a fixed 13 mm lens (45° x 37°) and a similar microbolometer sensor array that captures thermal radiation in roughly the same long-wave range (7.5–13 μm) at frame rates of ~7.5 Hz. This camera has an operating range of −25° to +135 °C and is slightly more sensitive to small changes in thermal emissivity (< 0.05 °C / 50 mK at temperatures near 30 °C). Also, at the University of Iowa, we use a FLIR A35 camera with slightly different specifications (320 × 256 sensor array, 48° x 39° fixed 9 mm lens; −40° to +550 °C range).

For recordings and analysis, we set the lower display limit to 2 °C below the ambient thermal emission of dry filter paper on the cage floor. Doing so provided optimal thermal contrast for identifying the border between the convective cooling of void spots relative to the dry filter paper surrounding them. We also standardized the upper display limit for all recordings at 38 °C, which is slightly higher than the core body temperature and thermal emission of mice and, therefore, of freshly voided urine.

For our recordings, we left the thermal camera and analysis software emissivity values at the default setting of 0.95 and did not perform reflectance or emissivity calibrations. The goal of our assay is accuracy in the temporal and spatial dimensions, neither of which require accurate absolute temperature values. All surfaces vary in their emissivity and reflectance, which means that any two surfaces differing in emissivity or reflectance, such as paper (high thermal emissivity; low thermal reflectance) and polished metal (moderate emissivity; high reflectance) will falsely appear to have different temperatures purely on the basis of these surface properties unless labor-intensive calibrations are performed separately, for each surface. That is, accurately measuring the temperature of any material requires first determining and calibrating to the precise emissivity of its surface and then measuring and correcting for the reflectance of that surface relative to a fixed position (Bernard et al., 2013). In our MVT assay, images contain both movement and diverse surface elements (mouse fur, dry and wet filter paper, plastic cage material, etc.), and our endpoints rely on *relative* differences in temperature, not absolute temperature values, so we do not calibrate emissivity or correct for reflectance.

In theory, wide fluctuations in ambient temperature could skew our estimates of void-volume because we calculated these from the area of

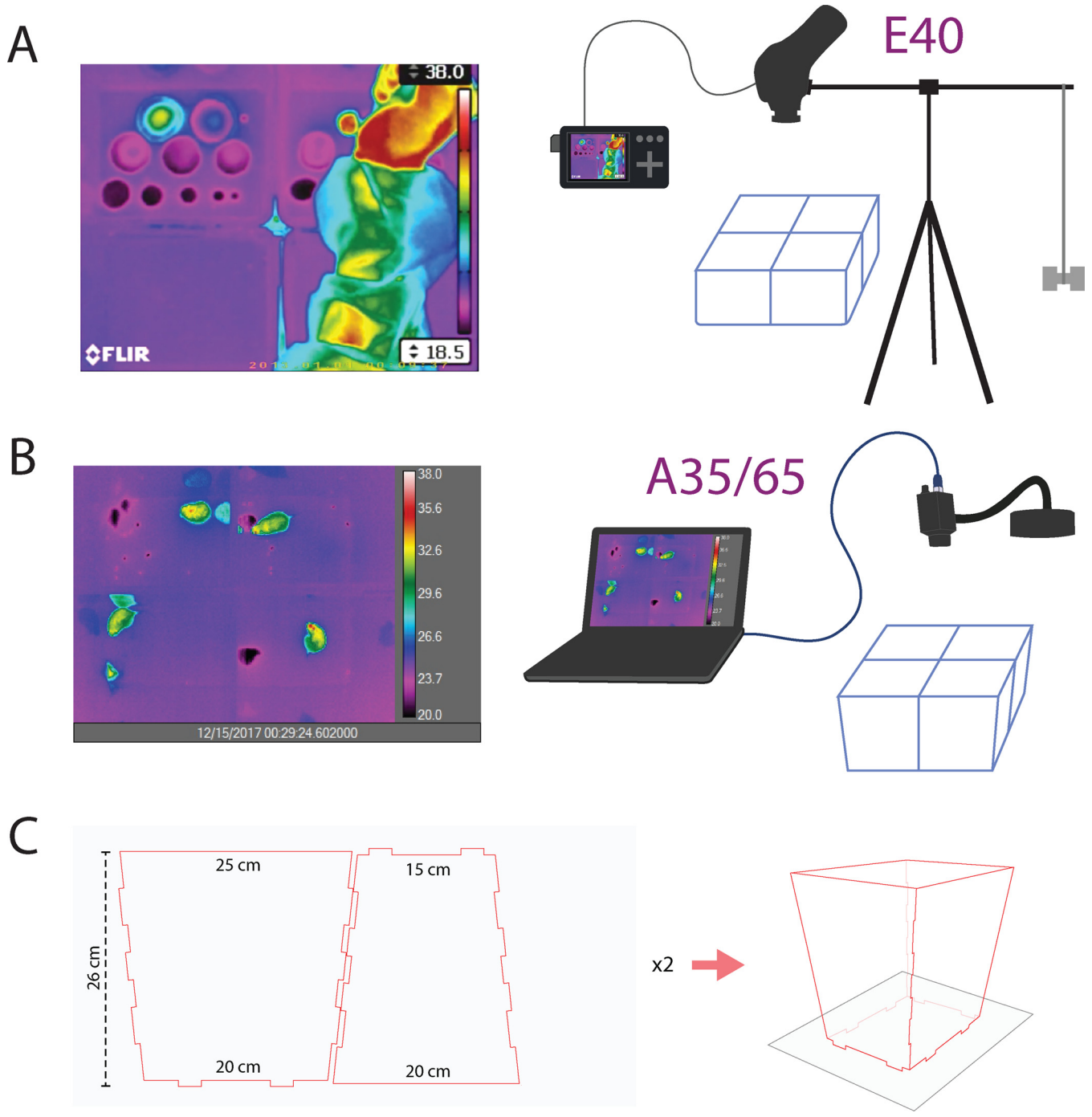

Fig. 1. (a) MVT imaging setup with a FLIR E40 camera mounted horizontally above 4 mouse enclosures, with RCA video output to a digital recorder, which encodes AVI video to a microSD card. (b) MVT imaging setup with a FLIR A35 or A65 camera, connected via gigabit Ethernet connection to a laptop running ResearchIR software. (c) Enclosure pattern for laser-cut acrylic sheets (24 × 12 × 3/16 inch) to produce chamber walls that angle slightly outward, allowing an improved camera view of the inner cage corners. Two sheets cut with this pattern yield walls for one enclosure. Up to four enclosures sit atop a large sheet of blotting paper, and void spots along the cage walls and corners diffuse radially within the paper, beneath the enclosures.

each void spot, and this area measurement was performed in images with temperature thresholds set relative to the ambient thermal emission of filter paper at the outset of each session. Fortunately, however, the ambient temperature at BIDMC is tightly controlled on a room-by-room basis and per our building engineers, the procedure rooms in which we performed most recordings at have stable temperatures of 73.00 ˚F (23 ˚C) or 69.98 ˚F (21 ˚C); digital thermostat archives from each room showed year-round temperature fluctuations with less than 1 ˚C maximum amplitude. Further, across hundreds of recording sessions, we have not encountered fluctuations in background temperature outside this range (measured from dry filter paper and plastic cage walls). The background temperatures in our recordings fluctuated slowly, with an amplitude never greater than +/- 1 ˚C. Ambient temperatures at the University of Iowa varied gradually and more widely (+/- 1–2 ˚C), without significantly impacting the contrast of liquid spots relative to surrounding paper.

Data acquisition. For initial recordings with the E40, we built a horizontal tripod to mount the camera facing down above four recording cages (Fig. 1A). Atop a standard 54″ camera tripod (Targus) we attached a horizontal camera bar (ALZO digital), adapting the 3/8″

female thread on the E40 camera to the bar's standard 1/4″ camera thread, and we suspended a 500 mL bag of saline on the opposite end of the bar as ballast. Before placing mice in cages, we centered the camera lens directly over the central corners of our four-cage array to minimize IR light blockage by the inner cage walls.

For subsequent recordings with A65 and A35 cameras, which are lighter, we used the gooseneck adapter in the "workbench" kits for each camera (FLIR; Fig. 1B). We placed a weighted base on a shelf above the array of test cages, then adjusted the gooseneck to face the camera straight down and center it directly above the central cage corners. Immediately before placing mice in the test cages, we focused the camera on chow pellets placed at the center of each enclosure, then at the beginning of each MVT recording, we refined the focus on the thermal contrast of resting mouse tails to most closely approximate the focal depth of the filter paper. Along 1–2 cm of the inner corner, less than 1 cm of the floor was blocked from the camera's view in our initial enclosures, and in subsequent recordings we used enclosures with tapered walls to eliminate this issue. To ensure that we measured any void spots along the inner cage walls in their entirety, for our earlier recordings, at the end of each test and immediately after returning each mouse to its home cage, we flipped open the top half of the enclosure and centered its base beneath the camera to reveal any edges and corner void spots that were partially obscured earlier in the recording.

Similar to camera choice and mounting hardware, our digital recording strategy evolved with experience. Initially, we attempted to record data directly on an SDHC card in the E40, using its on-board MP4 encoding, but recordings longer than 5–10 min occasionally resulted in corrupt video files. FLIR engineers noted that the E40 was not designed to record videos longer than seconds to minutes, so we switched to connecting the E40's component video-out port to a digital video recorder (iRecord; Stellar Labs, MCM Electronics #33-11690), which encodes AVI compressed video onto a microSD card, with an average ~2 GB file size for each 2 h session. We stored all recordings redundantly on a network and portable hard disk, and transferred video files to a MacBook for review and analysis. In contrast to the E40, the A65 and A35 cameras have no on-board recording ability. Instead, they are powered and controlled via gigabit Ethernet over a Cat6 cable connection to a laptop PC running ResearchIR (FLIR). This software generates uncompressed, full-spectrum radiometric SEQ files, which at 640 × 512 pixels and ~7.5 fps (A65) results in ~35-40 GB file size for a 2 h recording. We archived these large, raw thermal data files, but also encoded WMV files (200–300 MB per 2 h) using ResearchIR's export encoder set at ~85% quality), and used VLC (VideoLAN) for video review and analysis.

Void spot calibrations. Analogous to *post hoc* measurements of void spots in filter paper (Sugino et al., 2008; Yu et al., 2014), we generated calibration data for determining volume from the area of each "thermal void spot." We first generated calibration curves for 0.9% saline at two different temperatures (~25 °C room temperature and ~36 °C body temperature), then compared saline to mouse urine, and finally, compared calibration curves for each between filter paper and blotting paper.

For regression analyses in Fig. 2C, sterile 0.9% NaCl was left at room temperature, or warmed to 38 °C by wrapping a 15 mL tube in a warm pad for 15 min, or kept in a 40 °C water bath. After light handling, the tube surface temperature measured by video thermography ranged 33–36 °C for the warmed saline and 25–26 °C for the room temperature tube. Then, using standard, calibrated laboratory pipettes, we ejected saline from each tube onto dry filter paper in side-by-side empty enclosures, in aliquots ranging 10 µL - 1 mL. We tested both the GB004 filter paper and 360 gsm blotting paper (above) and shifted to using exclusively the blotting due to its superior durability. For the analyses in Fig. 2A and B, we kept the saline tube at 40 °C in a water bath, and we ejected warm saline at temperatures ranging 35–39 °C onto 360 gsm blotting paper. Our area-volume calibration results differed from a recent study using similar paper (Yu et al., 2014), highlighting the importance of repeating and comparing these calibrations after any change in experimental setup.

Next, to test whether the osmolality or solute composition of urine alters diffusion distance, we compared thermal spots from mouse urine with 0.9% saline. We pooled urine, collected from 98 mice of various genetic backgrounds by holding each mouse over wax paper and massaging the bladder (if the mouse did not void spontaneously), then pipetting the urine from the wax paper into a 1.5 mL tube (Kurien and Scofield, 1999). Individual urine samples, ranging 10–250 µL, were stored at −20 °C, then thawed, centrifuged (10 s at 5000 rpm), and pooled into a 15 mL conical tube for a total volume of ~ 5 mL amber fluid. The osmolarity of this pooled sample was 1765 mOsm (10 µL subsample, measured with a vapor osmometer), roughly 6-fold higher than 0.9% saline (~300 mOsm). The sodium concentration of this pooled urine sample was approximately 90 mmol (calculated from values of 1500 and 1300 ppm in separate, 150 µL sub-samples measured with an ion-selective membrane: B-722 LAQUAtwin sodium ion meter; Horiba; Kyoto, Japan), which is slightly less than the ~150 mmol sodium concentration of 0.9% saline. These values are consistent with what is known about the highly concentrated, sodium-retentive excretory physiology of mice (Parfentjev and Perlzweig, 1933). After warming both the pooled urine and 0.9% saline to 38 °C, we pipetted aliquots of each onto clean filter paper during live video thermography (as above) in side-by-side cages. Thermal (E40) camera recordings continued for more than 30 min after ejection of all calibration spots.

Also, because we observed variable sizes and rapid cooling with smaller calibration spots (< 50 µL), we performed an additional set of calibration tests in the range of 1 µL–48 µL (Fig. 3). For this test, we ejected PBS (35–39 °C) onto 360 gsm blotting paper and recorded for 4 h using a FLIR A35. Finally, to compare thermographic area-volume estimates with estimates obtained by visually tracing the same spots *post hoc*, we pipetted a series of warm saline spots (5, 12, 25, 50, 75, 100 µL) onto 360 gsm blotting paper. After any subsequent changes in camera (A65 or A35) or room/setup, we performed a new volume-area calibration curve with saline spots across the range 60–600 µL.

Data analysis and presentation. In ResearchIR, we reviewed thermal SEQ files and either performed data analysis directly in this program or exported them to WMV format with clock time and a thermal scale in every frame. The AVI videos from our E40 recordings already had a thermal scale from the camera, with a timestamp appended by the recording device. All videos were opened in VLC for initial review and analysis. In all recordings, temperature display thresholds were set to a high of 38 °C (just above the maximum temperature of mouse body surfaces and freshly voided urine) and low of 19–22 °C (2 °C below the average background temperature in a recording) with a linear scale and a rainbow color palate, which boosts contrast sensitivity for detecting voids and helps sharpen the borders of void spot for area measurements.

We reviewed each recording at high speed to record the time of each void and to identify an optimal frame with an unobstructed view for measuring its area of diffusion. We recorded the time of voiding as the first frame with warm, freshly voided urine immediately upon the mouse's first movement away from the void. In rare cases, a mouse hovers over and obstructs the camera's view of a small void, which delays the time recorded past what is likely the actual void time by one or more seconds. The frame captured for measuring the area of a void spot was typically 10–15 min after the time of voiding, when the void spot reached a stable, maximum area and stopped expanding. We picked a frame with a stable background temperature, typically just after a NUC (non-uniformity correction) on the camera, to minimize the effect of thermal sensor "drift" obfuscating the otherwise sharp border between void spot and background.

A full-size video frame containing each spot was captured and converted to 8-bit grayscale in ImageJ. Each void spot border was fitted using the ellipse tool, and its pixel area was calculated using the Measure tool. To convert pixel area to cm^2, we measured the pixel area

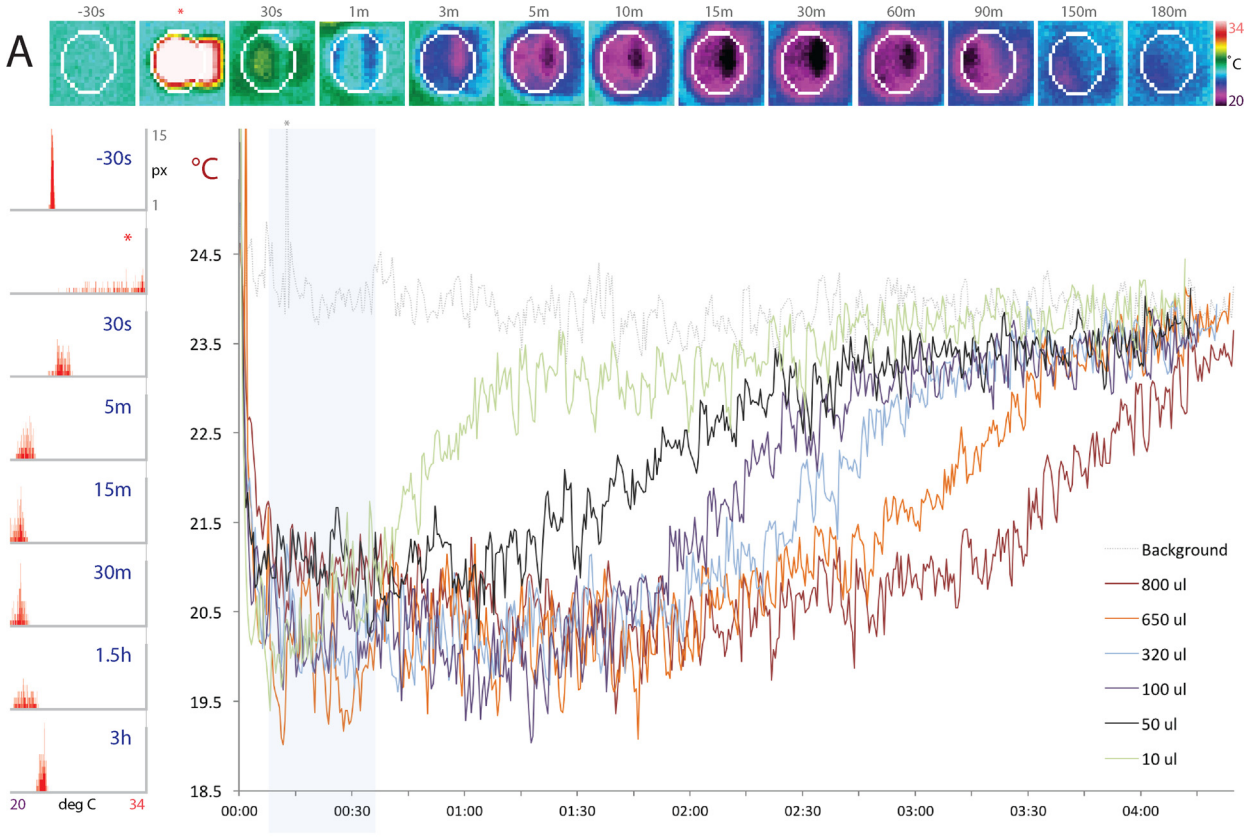

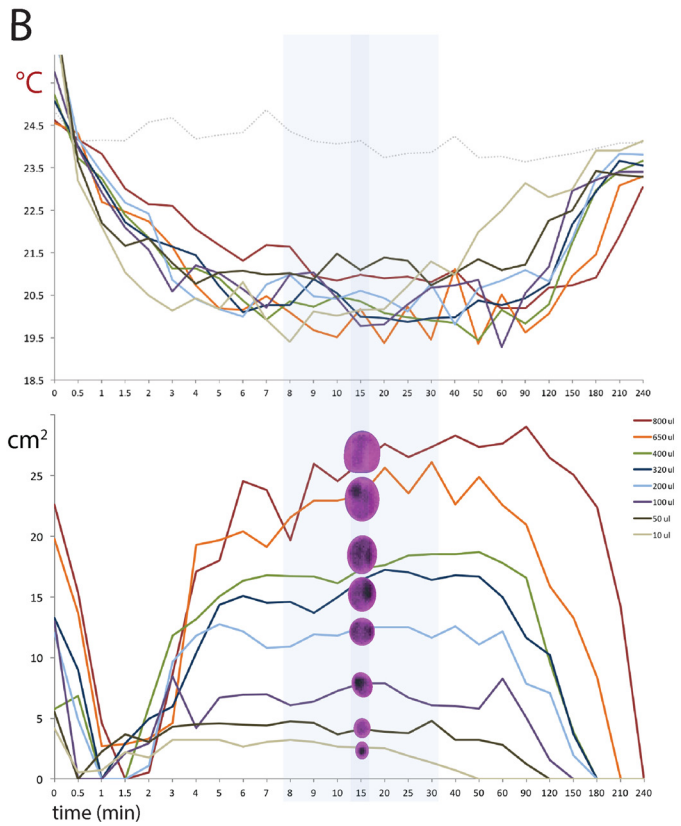

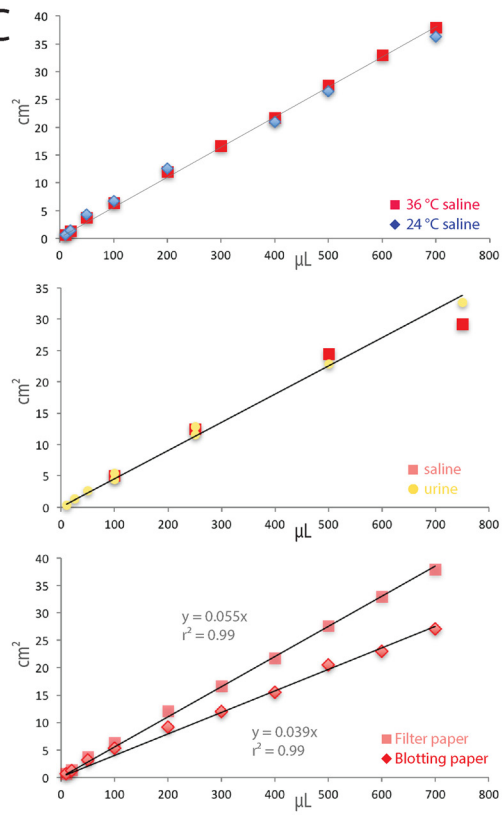

(caption on next page)

Fig. 2. Thermography calibration data with A35 (A–B) and E40 (C) cameras. (A) Top row images show the evolution of a thermal void spot in blotting paper from 30 s prior to 400 μL of warm saline ejection (*) through radial spread and cooling (30 s - 90 min), then delayed re-warming back towards the ambient temperature (150–180 min). At right is a thermal pseudocolor scale (20–34 °C). The left-hand column of histograms shows, for all pixels inside the white region of interest (ROI) in the top row of images, the distribution of pixels at each temperature (20–34 °C) across the same 3 h span: initially at the ambient temperature, transiently warm upon fluid ejection, then cooling several degrees, followed by a gradual re-warming back towards the ambient temperature. The large graph (at right) shows the minimum-temperature trend across a 4 h recording for calibration fluid volumes ranging 10 μL–800 μL, encompassing the range of volumes voided by awake mice. Notice that smaller spots re-warm sooner, while larger spots remain cool longer, but all spots cool to a stable, low temperature for roughly 10 to 30 min after ejection (blue highlighted region). (B) Temporal evolution of void spot temperatures (top) and measured areas (bottom) across a 4 h span for calibration spots ranging 10–800 μL. The region of thermal and size stability for most spots is highlighted in blue, and a darker blue stripe indicates 15 min timepoint optimal for measuring spots. (C) The radial spread of known volumes of saline in filter paper is similar at room temperature (24 °C) and body temperature (36 °C, top), as is the spread of mouse urine relative to saline (both 36 °C, middle), but paper type alters the slope of the area-volume relationship, with saline (36 °C) spreading further in filter paper than in blotting paper (bottom graph).

of each cage floor in ImageJ, averaged them together, and divided this number by the actual cage floor area (14 × 20 cm = 280 cm^2 in our initial setup with the E40 camera; 15 × 20 cm = 300 cm^2 in our current configuration). We used this constant to convert the pixel area of each thermal void spot in each recording to cm^2, which allowed us to estimate voided volume, using volume/area calibration data described above. We then plotted the initial fluid volume ejected from the pipettor (x) against the thermal void spot area in cm^2 (y) and performed a simple linear regression in Microsoft Excel with the y-intercept set at 0. We used the inverse slope of this linear regression to estimate urine volume from subsequent measurements of mouse void spots. For *post hoc* optical tracings of saline calibration data, we outlined each liquid spot and used a 10 cm scale bar drawn onto the filter paper for spatial calibration using the "Analyze > Set Scale" function in ImageJ.

Histograms and temperature-time data for individual void spots were generated in ResearchIR, and these data were exported to Excel for analysis and figure preparation. We used Adobe Photoshop CS3 to edit bitmap images, Illustrator CS3 to layout final figures, and iMovie (Apple) to edit the supplemental video, showing a typical mouse void in an MVT recording with the E40 camera.

Mouse position analysis. We exported ResearchIR thermography files (SEQ format, sampled at 3 frames per second) from four MVT sessions (containing n = 8 mice, recorded twice each on subsequent days) into WMV format. We imported WMV video files into EthoVision (Noldus), designating each cage as an independent arena. Each mouse was tracked for 2 h. This allowed us to plot the distance a mouse moved at any time during the MVT session. The distance traveled by each mouse, per video frame (in cm), for the 10 s before and after each void, was aligned to the appearance of warm urine in the source video. We then plotted 36 examples where EthoVision tracking did not lag the mouse position by more than 1 s (per manual review of the EthoVision tracking dot), as well as the average time-course.

We used the EthoVision heat map tool to highlight areas where the mouse spent the most time in red, and areas where the mouse spent less time, such as just walking through, in blue or black. To produce the images in Fig. 5D, we imported a grayscale image stack, containing one frame per 30 s from a 2 h MVT session, into ImageJ, then Z-projected this stack into a single grayscale image using the mean intensity setting. In Photoshop, we overlaid this image as a separate layer atop the EthoVision mouse position analysis from the same MVT recording, and blended the two layers together, pseudocoloring the thermal imaging (void spots) layer yellow.

3. Results

Thermal spot analysis. Our thermal images have relatively uniform backgrounds, reflecting ambient temperatures of 21–24 °C. Void spots appear suddenly, with high thermal contrast (> 10 °C above the background temperature), making it easy to time each void. Each void spot cools to ambient temperature within a minute, while spreading radially in the paper, then continues cooling until it reaches ~3 °C below the ambient temperature. Understanding dynamics of this thermal and spatial evolution is important for accurately measuring and deriving the urine volume, so we first show the changes in temperature and void spot area after ejecting known volumes of warm saline (Fig. 2A-B). Cool thermal contrast between a void spot and the dry paper surrounding is the basis for identifying it, detecting its edges, and measuring its area, so we analyze spots at a time when their temperature and size are predictably stable. That is, void spot measurements ideally should happen when radial growth finishes, but also when the spot has a predictable, stable temperature relative to surrounding filter paper.

The appearance and evolution of saline calibration spots was qualitatively similar to mouse void spots described below. First, each spot loses heat rapidly, cooling in less than 1 min from warm to less than ambient (23–24 °C) temperature, then gradually (5–10 min) cools to a minimum temperature that is several degrees below the ambient temperature. All but the smallest spots (< 50 μL) maintain this temperature minimum for an hour or longer. Spots 10–50 μL begin re-warming toward the ambient temperature in less than 1 h, while spots larger than ~500 μL remain below the ambient temperature for more than 2 h.

Over the same time span, the areas of saline calibration spots (Fig. 2B) dip transiently, which is an artifact of losing thermal contrast as their temperatures transiently cross the ambient temperature. Spot areas then increase for several minutes until peaking between five and thirty minutes later (light blue area in Fig. 2A–B). The areas of small spots can peak as early as 3–10 min (10 μL spot), while larger spots peak later. For, example, an 800 μL spot's growth slows by ~10 min, but may not peak for 30–90 min. By directly comparing the temporal evolution of both the temperature and area of each spot, we chose a post-void time interval of 15 min (blue line in Fig. 2B) to optimize the accuracy and consistency of volume estimates for the typical range of void spot sizes we see in awake, behaving mice (~100–400 μL).

Next, we tested whether fluid temperature (24 vs. 36 °C saline), fluid composition (saline vs. mouse urine), or paper type (filter vs. blotting paper) meaningfully alters the area-volume relationship underlying our estimates of urine volume. Fluid temperature did not alter the area of saline spot diffusion, as the area-volume relationships of saline calibration spots were virtually identical at 24 °C and 36 °C (Fig. 2C). The slope (area/volume) differed by less than 4% (0.053 vs. 0.055 $cm^2/\mu L$ for 24 vs. 36 °C), with a strong linear correlation ($r^2 = 0.99$, separately and together). Likewise, despite substantial differences in osmolality and sodium concentration, pooled mouse urine and warm saline had similar areas of diffusion with similar, linear area-volume relationships ($r^2 = 0.99$). The one factor that noticeably altered the area-volume slope was the paper flooring type (Fig. 2C). Blotting paper showed slightly less total diffusion, with on average ~20% smaller thermal spots. This necessitates separate conversion factors to estimate urine volume (in μL) from a void spot area (in cm^2) for experiments on filter paper relative to our on-going work using blotting paper. In either case, we multiply the area by the inverse slope of the area-volume regression in our saline calibration data (range 0.039 - 0.055 $cm^2/\mu L$).

We also examined the temperature and temporal dynamics of smaller calibration spots, in the range of 1–48 μL (Fig. 3). As above, small spots rewarm more rapidly than larger spots (Fig. 3A), and the

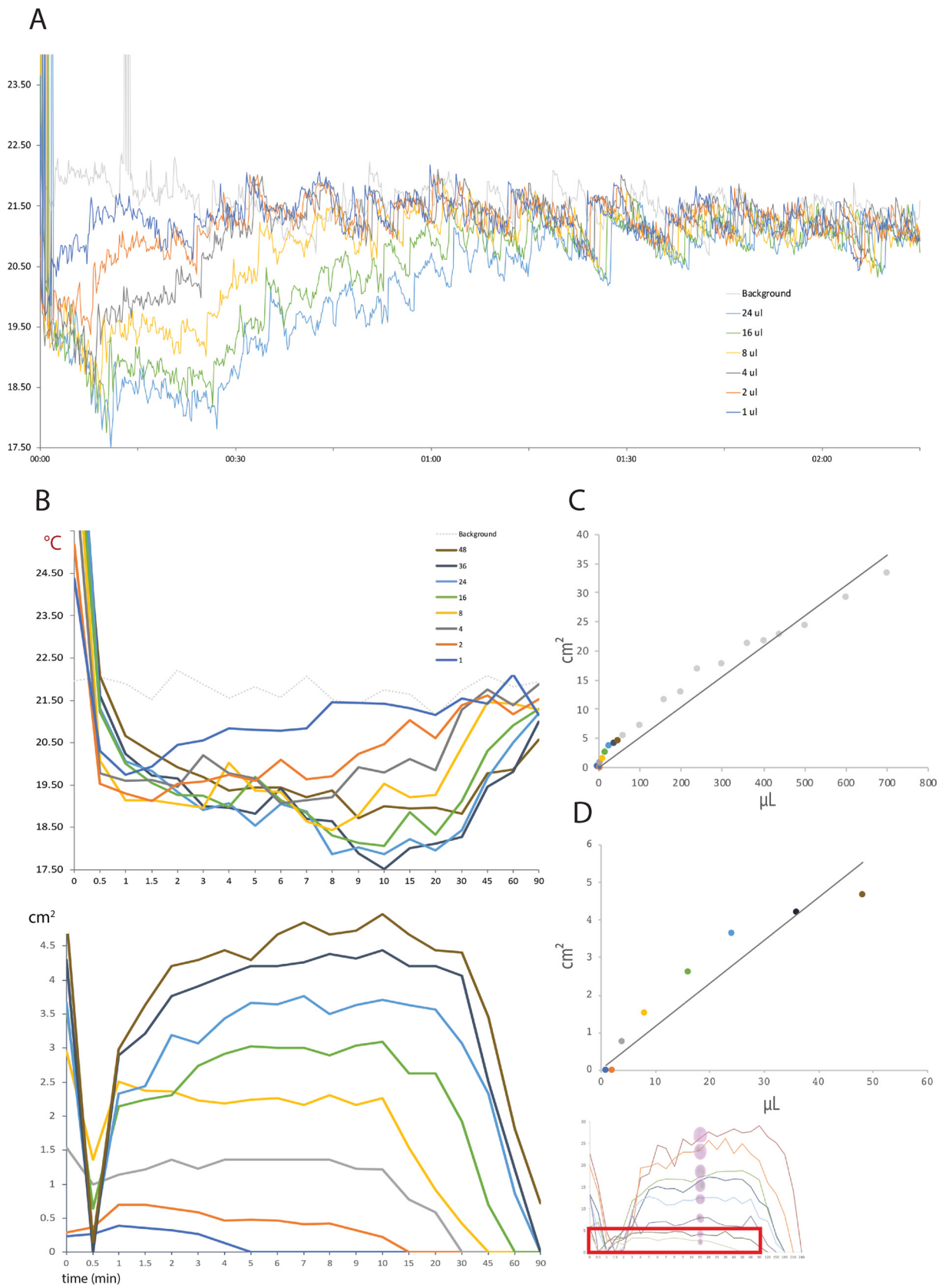

Fig. 3. Calibration data for small thermal void spots in blotting paper (A35 camera). (A) Minimum-temperature trend across a 2 h recording for calibration fluid volumes ranging 1–48 µL. (B) Temporal evolution of fluid spot temperatures (top) and measured areas (bottom). The faded graph (bottom-right) refers to the area measurements 10–800 µL in the previous figure, with a red box highlighting the smaller volume range in this Figure. (C) Area-volume calibration data in the overall range 1–800 µL is linear (R^2 = 0.95; y = 0.052x), but for very small spots in the range 1–48 µL (D), the area-volume relationship is less linear (R^2 = 0.89; y = 0.115x).

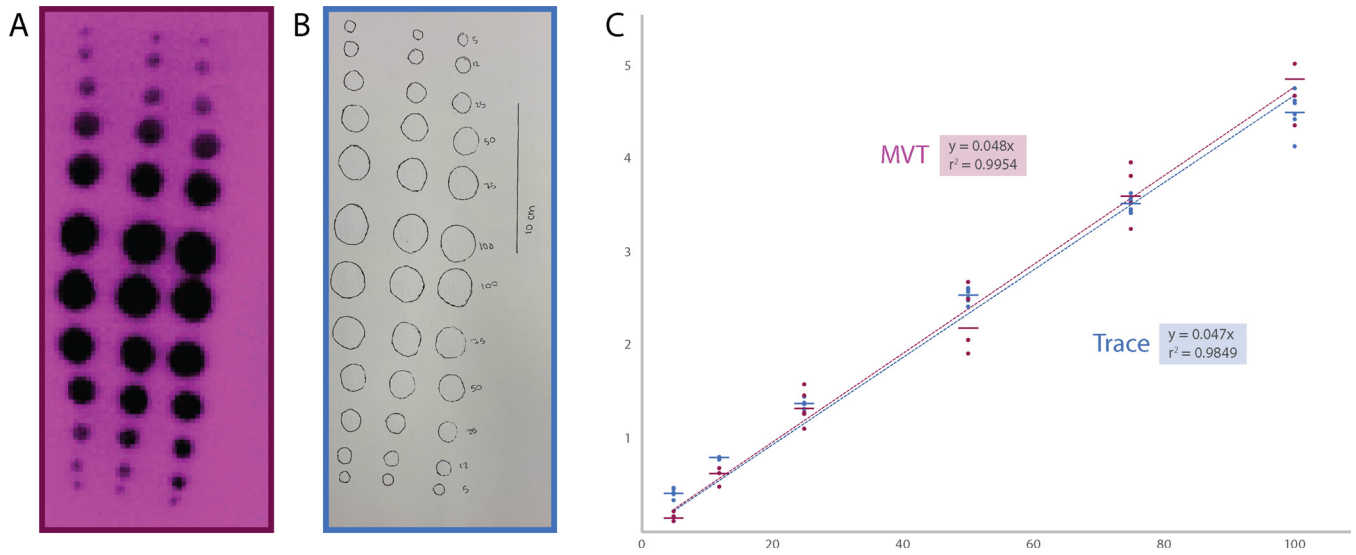

Fig. 4. (A–B) Thermographic (purple) and *post hoc* tracing (blue) methods for measuring spot area yield similar area-volume calibration curves (C).

smallest (1–2 μL) disappear entirely into the ambient temperature background within 5–15 min (Fig. 3B). Surprisingly, in the range of 1–48 μL, we observed a non-linear relationship between volume and spot areas when measured at 15 min (Fig. 3D), possibly due to the technical difficulty of accurately measuring smaller pixel areas as spots are more rapidly cooling toward the ambient temperature.

Finally, we compared the area-volume relationship of saline calibration spots (5–100 μL) measured with MVT (Fig. 4A) and then traced on the filter paper *post hoc* (Fig. 4B). Manual tracing yielded a strong linear correlation (r^2 = 0.9849) similar to our MVT procedure (r^2 = 0.99954; Fig. 4C).

Mouse imaging: basic observations. The temporal and spatial characteristics of thermal void spots in live mouse recordings (Fig. 5) are similar to the saline calibration data shown in Figs. 2. Mouse void spots maintain cool thermal contrast ~3 °C below the ambient temperature for typically the remainder of a 2 h MVT recording session, and across a range of sizes they stabilize in both temperature and size by ~15 min, similar to saline calibration spots.

The surface temperatures of mice range from ~27 °C along the trunk fur to 35–37 °C over the eyes, interscapular region, and inner ears. The tail and limb can be as low as the ambient temperature (23–25 °C), but warm occasionally to 35–37 °C, reflecting dynamic autonomic control of peripheral vasomotor tone (Geerling et al., 2016; Rudaya et al., 2005). At the beginning of a test, mice explore the chamber for up to 15–45 min. After that, most mice spend the majority of their time in one corner, resting and sometimes grooming. Occasionally, they venture from this corner to explore the cage or void.

Mice also defecate frequently, typically 10–20 times per 2 h recording. Unlike the behaviors consistently associated with micturition (below), we did not identify any stereotyped behaviors before, during, or after defecation. Rather, stools appear at random, usually while a mouse is exploring its cage or grooming. That is, defecation does not appear to be an overtly "continent" behavior in this species, in that it does not entail behavioral complexity or stereotypy. Though the cool thermal contrast of stools could confound thermal void spot analysis, distinguishing stools from urine is straightforward; urine emerges at roughly core body temperature, whereas stools emerge at relatively cool temperatures, within a few degrees of ambient temperature, possibly a consequence of residing nearer the ~27 °C posterior body surface, closer to the trunk or ambient temperature than to core body temperature. To identify these small, dark objects as stools (rather than small void spots), we use the following criteria: (a) the shape is that of a small bean or kidney that does not expand (in contrast to void spots, which expand radially to form an ellipse); (b) stools often move when contacted by the mouse, whereas void spots remain fixed in place throughout the recording; and (c) stools remain dark (cooler than ambient temperature) much longer than similarly sized (small) voids, which re-warm to room temperature and vanish from the thermal image in less than an hour (Figs. 2 and 3). The rare occurrence of semi-solid stool could present a challenge because its liquid content can spread into the filter paper with an appearance similar to that of a small void spot. Across many MVT recordings, non-solid stools were very rare, but we make a visual note of any semi-solid stools at the end of every recording so that none are inadvertently counted as void spots.

Stereotyped voiding behavior. Across > 1000 observations in > 100 mice, most male and female mice void rarely during MVT. The typical range is 1–3 and rarely as many as 5–6 voids per 2 h test. Mouse voiding behavior is continent and highly stereotyped (**Supplemental Video**). The voiding behavioral sequence typically begins with the mouse suddenly leaving its resting or grooming stance in the "home" corner. It explores, rears, paces, and/or grooms for several seconds or up to a few minutes, then walks to an opposite or adjoining (non-home) corner of the enclosure. There, the mouse quickly spins around to face away from the wall and assumes a visibly relaxed posture (not rearing, hunching, or stretching), without any apparent movement for several seconds (Fig. 5C). Often, the tail lifts slightly. Then, after warm (~35–37 °C) urine emerges from beneath (see **Supplemental Video**), the mouse abruptly resumes a normal, waking posture and walks away from the fresh urine. In the subsequent minutes, sometimes immediately after walking away, mice usually return to sniff the fresh void then walk away again. Some mice repeat this return-and-sniff sequence once or twice more, each time increasing other activities between return trips (grooming, rearing, exploring, and/or pacing). Within minutes, and sometimes immediately after voiding, the mouse returns to its "home" corner to rest.

4. Discussion

We developed a new, non-invasive technique for live-monitoring mouse voiding behavior. This technique, MVT, reliably records the timing, location, and volume of voiding, as well as mouse behaviors. MVT makes it possible, and practical, to perform live neuroscience experiments with high temporal resolution (Verstegen et al., 2019). It can complement or perhaps supplant older assays for voiding in awake, behaving mice. After addressing technical advantages and limitations of MVT, we discuss our observations on the voiding behavior of awake,

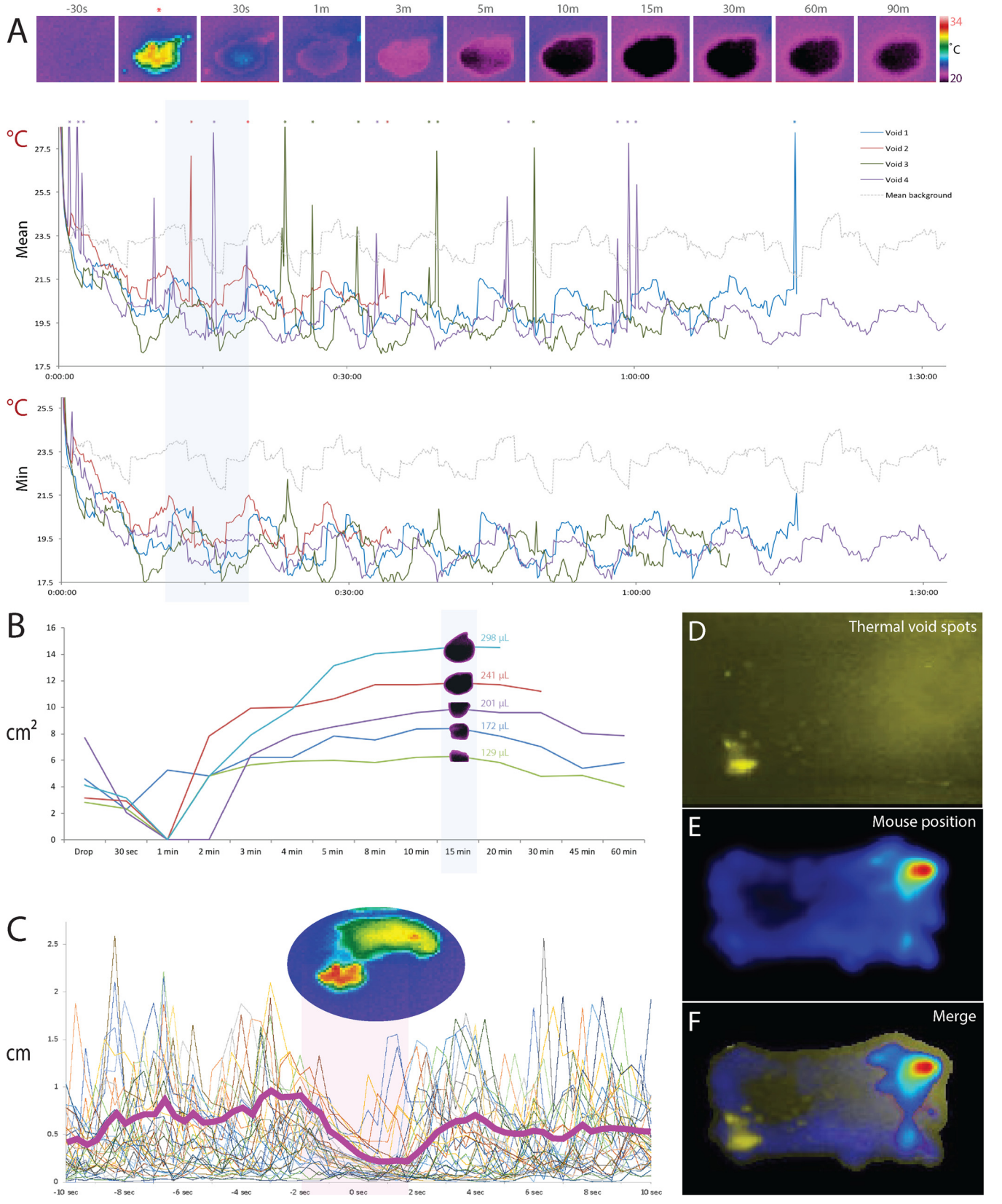

(caption on next page)

untethered mice relative to previous reports and propose future applications for MVT that should facilitate translational studies of the neural circuits that control urinary continence and voiding.

Limitations. While MVT has many advantages over other, more invasive and less informative methods, there are limitations that should be considered. One of these limitations is the time required for data analysis. Setting up a 2 h MVT trial requires less than 20 min of investigator effort, and a recording with 4 mice can be scored for void

Fig. 5. Mouse void spot analysis. (A) Top row images show the evolution of a thermal void spot, beginning 30 s prior to the void (*) and continuing through the radial spread and cooling of the void spot (30 s - 90 min). At right is a thermal pseudocolor scale (20–34 °C). The top graph shows the *mean* temperature across all pixels in four typical void spots (4 voids of n = 4 mice from two MVT cohorts). Void times are aligned to common time-zero and temperature data continue to the final frame of each 2 h MVT recording. Spikes in the mean temperature on this graph (indicated by *) correspond to the warm mouse crossing through the pixel boundary of the void spot. The lower graph shows minimum temperature evolution of the same void spots, which blunts the appearance of these temperature spikes. (B) Evolution of the measured area (cm^2) of typical thermal void spots (5 spots from n = 5 mice across two MVT cohorts). Blue background indicates the 15-min time point we chose for optimal temperature and size stability across a wide range of void volumes based on calibration data in Figs. 2–3. (C) Motion-tracking analysis of thermal videos (36 voids from n = 8 mice across four MVT recording sessions) reveals that mice pause for roughly 2–4 seconds around the time of voiding. Bold magenta line indicates the average change in position (cm per 3 Hz video frame). (D) Two-hour Z-projection of inverted thermal imaging data shows preferential voiding in one corner. (E) Heat map showing the distribution of the mouse's location across the 2 h MVT session. The overlay in (F) in this typical example reveals that the mouse spent most of its time in one corner (upper-right), but voided primarily in a separate corner (lower-left).

timing and location in ~10 min. However, capturing frames and measuring the area of each void spot can require up to an additional hour, depending on the number of voids. In the future, software automation could accelerate this process. As with any video assay, scoring mouse behaviors can be time- and labor-intensive, but we save time by using off-the-shelf software for mouse video tracking.

MVT is useful for recording up to several hours of mouse voiding behavior, but may not be well-suited for longer periods of time without water and bedding material. Without adaptations to the MVT assay, experiments requiring continuous measurement for many hours or days would require a different method, such as the UroVoid system or automated voided stain on paper (aVSOP) (Negoro et al., 2012, 2013). Also, mouse voiding varies across the 24 -h day (Negoro et al., 2013), so the circadian timing of MVT or any other voiding assay should be standardized and reported.

Another limitation is that we used only C57B6/*J* male mice. Voiding patterns may vary among mouse strains (Yu et al., 2014), though in testing a variety of genetic backgrounds in on-going experimental work, we have not yet seen qualitatively new or different patterns of voiding behavior on our MVT assay in most mice up to 7–8 months of age, relative to C57B6/*J*.

Rarely, video thermography is unable to capture a small void because a mouse blocks it from the camera view. This is uncommon because most mice spend the majority of their time in a home corner where they do not void. When mice do remain on top of a void, it is typically only for a couple seconds, after which the void is still above room temperature and easily identified. Even in cases where the mouse sits on top of a void for many seconds or minutes, the void cools below room temperature and can still be identified after the mouse walks away. However, if the void is small enough that it re-warms quickly to room temperature (also aided by the body heat of the mouse sitting on top of it), it may not appear on the video. The void can still be identified after recording and removal of the mouse from the filter paper, as there will be a small dried and discolored spot. This is rare, and we have only seen examples in experimental mice that are incontinent and not discussed in this paper. The aVSOP method can be used for experiments requiring more accurate volume estimates of very small voids < 50 µL (Negoro et al., 2012, 2013).

Another limitation of our new method is that it lacks control over or information about bladder pressure. A key feature of MVT is that it is non-invasive, and without catheterizing the bladder, we do not have ability to control or measure bladder volume or pressure. Further, while we can see when the mice void, MVT itself does not provide information about "non-voiding contractions" (NVC) of the detrusor muscle prior to urine ejection. We have had initial success (not shown here) combining MVT recordings with awake CMG, urethral sphincter EMG, and even wireless telemetric recordings of bladder pressure. These invasive techniques inevitably alter mouse voiding behavior. Also, bladder pressure recordings in awake, behaving mice are contaminated by noise from mouse movement, which can make pressure recordings difficult to interpret. Despite this, combining MVT with CMG could provide useful information about bladder pressure in relation to voiding behavior especially in disease models with small, unpredictable voids that empty only a small percentage of the bladder.

Finally, for EthoVision or other video behavioral analysis, a relatively low frame rate of affordable thermal cameras (~7 Hz for A35 and A65) may limit some analyses. This frame rate is more than enough for MVT void spot analysis, and we often down-sample prior to analysis to reduce file size. However, when these videos are run through EthoVision, mouse tracking often lags by one or more frames. This affected our movement analysis, as the software would sometimes take a second or two to catch up with the mouse after it stopped to begin voiding, but then would move with the mouse as soon as it was done voiding, making the pause in movement during the void appear up to a second shorter than it actually was. Some thermal cameras capture at higher frame rates, but another solution if better temporal resolution is needed would be to synchronize a standard video recording with the thermal camera, and use that video for motion tracking.

Comparison with established techniques and previous findings. We find that neither temperature nor osmotic composition of fluid has a significant impact on the area-volume relationship, but paper type does. This difference underscores the importance of re-calibrating the area-volume relationship for each new environment and paper type.

Our calibration data for the area-volume relationship of thermal void spots is similar to what was originally referred to as the VSOP (voided stain on paper) method by Sugino et al. (2008). Like us, they measured calibration spots across a wide range, 50–800 µL, and found a highly linear correlation between spot area and volume (R^2 = 0.9981). The slope of their area-volume calibration (y = 16.472x) differs slightly from ours (slopes ranging 18–25), probably due to differences in absorbent paper, which we find can alter the area-volume relationship by as much as 30%. In their study, mice were confined atop a wire grid (20 cm above filter paper), which may have altered mouse behavior, and the investigators outlined void spots manually on the filter paper post hoc, which also may contribute to measurement differences, relative to our digital MVT analysis. Another group of investigators also found a highly linear relationship (R^2 = 0.996), but with a reduced slope, which again may reflect differences in the absorbent paper composition (Yu et al., 2014). These investigators tested mice in their home cages and used ultraviolet imaging to outline void spots post hoc.

Importantly, with rare, smaller voids (less than 50 µL; areas less than ~4-5 cm^2) the area-volume relationship with MVT becomes non-linear, as shown in Fig. 3. For this reason, non-linear calibration and/or different post-void measurement times may be necessary when using MVT to study very young or incontinent mice.

Another study of mouse voiding used CMGs to show that dominant males, which mark extensively, frequently, and all over the cage, have residual bladder volumes of 0–140 µL, while subordinate males are more retentive, with bladder volumes of 630 µl to 1.02 mL (Pandita et al., 2000). We did not measure bladder volume before or after MVT, so we cannot comment on how full the average mouse bladder was at the beginning of the test or on their post-void residual volumes at the end of the test. Across many MVT tests, C57B6/J mice in our labs average ~2.5 voids totaling an average of ~400 µL per 2 h test, similar to previous estimates of ~4 voids totaling ~350 µL urine volume in C57B6/*J* mice using void spot analysis after 4 h tests (Bjorling et al., 2015; Yu et al., 2014).

Advantages over other techniques. Video thermography confers

several advantages that set it apart from previous techniques for measuring mouse voiding.

First, we can identify the exact time of each void. While this is possible with grid-bottom collection (UroVoid), it is not possible with post hoc void spot analysis. Similar to post hoc void spot analysis, we are able to see the exact location of each void, which gravimetric and CMG-based techniques do not allow. MVT allows us to differentiate between two voids that occur in the same location at different times. These voids are seen and analyzed independently during video playback. This is not possible with post hoc void spot analysis, in which the voids can be mistakenly counted as one larger void. With the other techniques, urine can be weighed, or void spots illuminated afterwards, but neither grid-bottom cages nor fluorescence, provide information on both timing and location.

Looking at time and location together in the same assay is already an advantage, but we are able to calculate the volume excreted as well. Our volume-area regressions show that there is a reliable relationship between the size of the void spot and the voided volume, similar to previous techniques. This provides us with the opportunity to analyze the timing and location of voids of varying sizes, as in a mouse with lower urinary tract symptoms like incontinence and urgency. Being able to understand the relationship between when, where, and how much a mouse voids has the potential to enhance real-time studies looking at how these aspects may change with experimental manipulations.

Analyzing the timing, location, and volume of voids adds to our understanding of mouse behavior around the time of voids. We are able to confirm previous observations that mice typically void on the edges and corners of their enclosures, and have a home corner where they do not void. We are also able to use video software to look at more complex behaviors including movement around the time of voiding.

One of the main advantages of video thermography is the fact that it is non-invasive. It does not require any surgical procedure, involves very little handling, and the enclosure the mouse is placed in does not cause physical discomfort. This creates many possibilities for combining MVT with other experimental techniques at the same time, or in sequence. Since MVT is non-invasive, it is well-suited for combination with an invasive technique, such as optic fiber implantations for neuronal stimulation, inhibition, or calcium imaging (Verstegen et al., 2019). If bladder pressure or sphincter activity are of interest, these also can be measured during MVT, by adding CMG or EMG recordings in awake mice.

Other thermal cameras. Our choice of the E40, then A65/A35 thermal cameras balanced cost-savings against performance considerations. We conducted preliminary tests with consumer-grade thermal cameras (FLIR C2/C3; Seek for iPhone) and found thermal measurement drifts and errors that were unfavorable for rigorous analysis. Also, the lower pixel resolution of most consumer-grade thermal cameras precludes overhead, simultaneous recordings of multiple mice. These low-resolution cameras may have adequate pixel resolution for recording individual mice, but at one camera per cage, the cost-savings of a low-end camera is less favorable, especially given the trade-offs in thermal sensor precision and stability. We have not tested the much more expensive, high performance “science” grade thermal cameras with non-bolometer sensors, which offer better pixel and temporal resolution, better precision and accuracy, and less thermal drift, but are cost-prohibitive for our work.

5. Conclusion

In summary, MVT is a robust, non-invasive, easy-to-implement way to measure void timing, volume, location, and associated behaviors in awake-behaving mice. It is well-suited for within-animal controls and repeat measurements, and can be easily paired with other techniques. This technique will help generate new understanding of neural circuits controlling continence, which is critical for developing new therapies for the large numbers of patients with urinary incontinence in our aging population.

Declarations of Competing Interest

None.

Acknowledgements

The authors wish to thank Warren Hill for feedback regarding void spot analysis, Steven Abbott for inspiration regarding the potential of thermal imaging for void analysis, Pavel Gorelik for help generating mouse enclosures, and Shane Heiney of the Iowa Neuroscience Institute neural circuits and behavior core for assistance with EthoVision motion tracking software.

Appendix A. Supplementary data

Supplementary material related to this article can be found, in the online version, at doi:https://doi.org/10.1016/j.jneumeth.2019.108449.

References

Andersson, K.E., Soler, R., Fullhase, C., 2011. Rodent models for urodynamic investigation. Neurourol. Urodyn. 30, 636–646.
Barrington, F.J.F., 1924. The effect of lesions of the hind- and mid-brain on micturition in the cat. Q. J. Exp. Physiol. 15, 81–102.
Bernard, V., Staffa, E., Mornstein, V., Bourek, A., 2013. Infrared camera assessment of skin surface temperature-effect of emissivity. Phys. Med. 29, 583–591.
Bjorling, D.E., Wang, Z., Vezina, C.M., Ricke, W.A., Keil, K.P., Yu, W., Guo, L., Zeidel, M.L., Hill, W.G., 2015. Evaluation of voiding assays in mice: impact of genetic strains and sex. Am. J. Physiol. Renal Physiol. 308, F1369–78.
Geerling, J.C., Kim, M., Mahoney, C.E., Abbott, S.B., Agostinelli, L.J., Garfield, A.S., Krashes, M.J., Lowell, B.B., Scammell, T.E., 2016. Genetic identity of thermosensory relay neurons in the lateral parabrachial nucleus. Am. J. Physiol. Regul. Integr. Comp. Physiol. 310, R41–54.
Hill, W.G., Zeidel, M.L., Bjorling, D.E., Vezina, C.M., 2018. Void spot assay: recommendations on the use of a simple micturition assay for mice. Am. J. Physiol. Renal Physiol. 315 F1422-F9.
Hou, X.H., Hyun, M., Taranda, J., Huang, K.W., Todd, E., Feng, D., Atwater, E., Croney, D., Zeidel, M.L., Osten, P., Sabatini, B.L., 2016. Central control circuit for context-dependent micturition. Cell 167 (73–86) e12.
Krohn, T.C., Hansen, A.K., Dragsted, N., 2003. Telemetry as a method for measuring the impact of housing conditions on rats' welfare. Anim. Welf. 12, 53–62.
Kurien, B.T., Scofield, R.H., 1999. Mouse urine collection using clear plastic wrap. Lab Anim. (NY) 33 83-6.
Negoro, H., Kanematsu, A., Doi, M., Suadicani, S.O., Matsuo, M., Imamura, M., Okinami, T., Nishikawa, N., Oura, T., Matsui, S., Seo, K., Tainaka, M., Urabe, S., Kiyokage, E., Todo, T., Okamura, H., Tabata, Y., Ogawa, O., 2012. Involvement of urinary bladder Connexin43 and the circadian clock in coordination of diurnal micturition rhythm. Nat. Commun. 3, 809.
Negoro, H., Kanematsu, A., Matsuo, M., Okamura, H., Tabata, Y., Ogawa, O., 2013. Development of diurnal micturition pattern in mice after weaning. J. Urol. 189, 740–746.
Pandita, R.K., Fujiwara, M., Alm, P., Andersson, K.E., 2000. Cystometric evaluation of bladder function in non-anesthetized mice with and without bladder outlet obstruction. J. Urol. 164, 1385–1389.
Parfentjev, I.A., Perlzweig, W.A., 1933. The composition of the urine of white mice. J. Biol. Chem. 100, 551–555.
Rudaya, A.Y., Steiner, A.A., Robbins, J.R., Dragic, A.S., Romanovsky, A.A., 2005. Thermoregulatory responses to lipopolysaccharide in the mouse: dependence on the dose and ambient temperature. Am. J. Physiol. Regul. Integr. Comp. Physiol. 289 R1244-52.
Sugino, Y., Kanematsu, A., Hayashi, Y., Haga, H., Yoshimura, N., Yoshimura, K., Ogawa, O., 2008. Voided stain on paper method for analysis of mouse urination. Neurourol. Urodyn. 27 548-52.
Verstegen, A.M.J., Klymko, N., Zhu, L., Mathai, J.C., Kobayashi, R., Venner, A., Ross, R.A., VanderHorst, V.G., Arrigoni, E., Geerling, J.C., Zeidel, M.L., 2019. Non-crh glutamatergic neurons in Barrington's nucleus control micturition via glutamatergic afferents from the Midbrain and hypothalamus. Curr. Biol. 29 (2775–89) e7.
Yoshiyama, M., Roppolo, J.R., De Groat, W.C., 1994. Alteration by urethane of glutamatergic control of micturition. Eur. J. Pharmacol. 264, 417–425.
Yu, W., Ackert-Bicknell, C., Larigakis, J.D., MacIver, B., Steers, W.D., Churchill, G.A., Hill, W.G., Zeidel, M.L., 2014. Spontaneous voiding by mice reveals strain-specific lower urinary tract function to be a quantitative genetic trait. Am. J. Physiol. Renal Physiol. 306, F1296–307.